Pis'ma v ZhETF, vol. 103, iss. 1, pp. 32 – 37 

# Quasi-one-dimensional quantum spin liquid in the $Cu(C_4H_4N_2)(NO_3)_2$ insulator

*V. R. Shaginyan*[+*1)], *V. A. Stephanovich*[× 1)], *K. G. Popov*[○], *E. V. Kirichenko*[∇]

[+] *Konstantinov St. Petersburg Nuclear Physics Institute, National Research Centre "Kurchatov Institute", 188300 Gatchina, Russia*

[*] *Clark Atlanta University, GA 30314 Atlanta, USA*

[×] *Institute of Physics, Opole University, 45-052 Opole, Poland*

[○] *Komi Science Center UB of the RAS, 167982 Syktyvkar, Russia*

[∇] *Institute of Mathematics and Informatics, Opole University, 45-052 Opole, Poland*

Submitted 23 November 2015

We analyze measurements of the magnetization, differential susceptibility and specific heat of quasi-one dimensional insulator $Cu(C_4H_4N_2)(NO_3)_2$ (CuPzN) subjected to magnetic fields. We show that the thermodynamic properties are defined by quantum spin liquid formed with spinons, with the magnetic field tuning the insulator CuPzN towards quantum critical point related to fermion condensation quantum phase transition (FCQPT) at which the spinon effective mass diverges kinematically. We show that the FCQPT concept permits to reveal and explain the scaling behavior of thermodynamic characteristics. For the first time, we construct the schematic $T-H$ (temperature–magnetic field) phase diagram of CuPzN, that contains Landau–Fermi-liquid, crossover and non-Fermi liquid parts, thus resembling that of heavy-fermion compounds.

DOI: 10.7868/S0370274X16010069

Recently, the striking measurements of the thermodynamic properties at low temperatures $T$ under the application of magnetic field $H$ on the quasi-one dimensional (Q1D) insulator $Cu(C_4H_4N_2)(NO_3)_2$ (CuPzN) have been performed [1]. The observed thermodynamic properties of CuPzN is very unusual and nobody expects that it might belong to the class of HF compounds, including quasicrystals (QC) [2], insulators with quantum spin liquid (QSL), and heavy-fermion (HF) metals [3–6]. Similar Q1D clean HF metal $YbNi_4P_2$ was recently experimentally studied, that reveals it has a Q1D electronic structure and strong correlation effects dominating the low-temperature properties, while its thermodynamic properties resembles those of HF metals, including the formation of Landau–Fermi-liquid (LFL) ground state [7]. These observations show that both CuPzN and $YbNi_4P_2$ can demonstrate a new type of Q1D Fermi liquid whose thermodynamic properties resemble that of HF compounds rather than the Tomonaga–Luttinger system. One of the hallmark features of geometrically frustrated insulators is spin-charge separation. The behavior of Q1D Fermi liquid (Q1DFL) is the subject of ongoing intensive experimental research in condensed matter physics, see, e.g., [1] and references therein. Q1DFL survives up to the saturation magnetic field $H_s$, where the quantum critical point (QCP) occurs giving way to a gapped, field-induced paramagnetic phase [1]. In other words, at $H = H_s$ both antiferromagnetic (AFM) sublattices align in the field direction i.e. the magnetic field fully polarizes Q1DFL spins. We will see below that in Q1DFL the fermion condensation quantum phase transition (FCQPT) plays a role of QCP, at which the energy band for spinons becomes almost flat at $H = H_s$ and the effective mass $M^*$ of spinons diverges due to kinematic mechanism. Thus, the bare interaction of spinons is weak [1]. In that case the original Tomonaga–Luttinger system can exactly be mapped on a system of free spinons, which low-temperature behavior in magnetic fields can be viewed as the LFL one [8]. Thus CuPzN offers a unique possibility to observe a new type of Q1D QSL whose thermodynamic properties resemble that of HF compounds like HF metals, including Q1D HF metal $YbNi_4P_2$ [7], quantum spin liquids of herbertsmithite $ZnCu_3(OH)_6Cl_2$ [6], and liquid $^3He$ [9]. Theory of Q1D liquids is still under construction and recent results show that the liquids can exhibit LFL, non-Fermi liquid (NFL) and crossover behavior [8, 10, 11].

1) e-mail: vrshag@thd.pnpi.spb.ru; stef@math.uni.opole.pl

In this letter we show that, contrary to ordinary wisdom, CuPzN can be regarded as an insulator belonging to HF compounds, while its thermodynamic properties are defined by weakly interacting Q1D QSL formed with spinons, and are similar to those of HF compounds. Here spinons are chargeless fermionic quasiparticles with spin 1/2. For the first time, we demonstrate that its $T-H$ phase diagram contains LFL, crossover and NFL parts, thus resembling that of HF compounds. To unveil the relation between CuPzN and HF compounds, we study the scaling behavior of its thermodynamic properties which are independent of the interparticle interaction. We demonstrate that CuPzN exhibits the universal scaling behavior, that is typical of HF compounds.

Upon transition to fermionic description, CuPzN is indeed represented by weakly interacting fermions. The description of weakly interacting fermion gas gives magnetization in terms of fermion number per spin $N/L = \int_0^\infty D(\varepsilon) f[\varepsilon-\mu(H)]d\varepsilon$, where $L$ is the number of spins in Q1D chain, $D(\varepsilon)$ is the density of states, corresponding to free fermion spectrum $\varepsilon = p^2/(2m_0)$ with $p$ is the momentum and $m_0$ is the bare mass. The chemical potential $\mu(H) = H_s - H$, and $f(x) = (e^x + 1)^{-1}$ is the Fermi distribution function [1, 12, 13]. The magnetization can be expressed as $M = M_s - N$ ($M_s$ is the saturation magnetization) or explicitly

$$M(H,T) = M_s - \frac{\sqrt{2m_0 T}}{\pi} \int_0^\infty \frac{dx}{e^{\left(x^2 - \frac{H_s - H}{T}\right)} + 1}. \quad (1)$$

Eq. (1) will be used below to calculate the differential magnetic susceptibility $\chi(T,H) = \frac{\partial M(T,H)}{\partial H}$. To calculate the specific heat $C(T,H)$, we need the internal energy $E$, which in the above approach can be calculated as follows

$$E(T,H) = \int_0^\infty \varepsilon D(\varepsilon) f[\varepsilon - \mu(H)]d\varepsilon, \quad (2)$$

so that $C(T,H) = \frac{\partial E}{\partial T}$. Within the framework of fermionic description, as it is seen from Eq. (1), CuPzN is indeed a weakly interacting fermions with simplest possible spectrum $\varepsilon = p^2/(2m_0)$, where (in atomic units) $\hbar = c = 1$. Near QCP taking place at $H = H_s$ and $T = 0$, the fermion spectrum becomes almost flat, and the fermion (spinon) effective mass diverges, $M^* \propto m_0/p_{\rm F} \to \infty$, due to kinematic mechanism, for the Fermi momentum $p_{{\rm F}H} \to 0$ of becoming empty subband. In case of weak repulsion between spinons the divergence is associated with the onset of a topological transition at finite value of $p_{{\rm F}H}$ signaling that $M^*(T) \propto T^{-1/2}$ [3, 14–17]. In accordance with Ref. [8], we suggest that the weakly interacting Q1DFL in CuPzN could be thought of as QSL, formed with fermionic spinons, constituting the Fermi sphere (line) with the Fermi momentum $p_{\rm F}$, and carrying spin 1/2 and no charge. For QCP occurs at $M^* \to \infty$, as we have seen above, we propose that QCP is FCQPT, at which the corresponding band becomes approximately flat [3–6].

In fermion representation the ground state energy $E(n)$ can be viewed as the Landau functional depending on the spinon distribution function $n_\sigma(\mathbf{p})$, where $\mathbf{p}$ is the momentum. Near FCQPT point, the effective mass $M^*$ is governed by the Landau equation [18, 4, 5]

$$\frac{1}{M^*(T,H)} = \frac{1}{M^*(T=0,H=0)} + \\ + \frac{1}{p_F^2} \sum_{\sigma_1} \int \frac{\mathbf{p}_{\rm F}\mathbf{p}_1}{p_{\rm F}} F_{\sigma,\sigma_1}(\mathbf{p}_{\rm F},\mathbf{p}_1) \frac{\partial \delta n_{\sigma_1}(\mathbf{p}_1)}{\partial p_1} dv, \quad (3)$$

where $dv$ is the volume element. Here we have rewritten the spinon distribution function as $\delta n_\sigma(\mathbf{p}) \equiv n_\sigma(\mathbf{p},T,B) - n_\sigma(\mathbf{p},T=0,B=0)$. The sole role of the Landau interaction $F(\mathbf{p}_1,\mathbf{p}_2) = \delta^2 E/\delta n(\mathbf{p}_1)\delta n(\mathbf{p}_2)$ is to bring the system to FCQPT point, where $M^* \to \infty$ at $T = 0$, and the Fermi surface alters its topology so that the effective mass acquires temperature and field dependences, while the proportionality of the specific heat $C/T$ and the magnetic susceptibility $\chi$ to $M^*$ holds: $C/T \sim \chi \sim M^*(T,H)$ [4, 5, 19, 20]. This feature can be used to separate the solutions of Eq. (3), corresponding to specific experimental situation. Namely, the experiment on CuPzN shows that near QCP at $H = H_s$, the specific heat $C(T)/T \propto \chi(T) \propto T^{-1/2}$ [1] which means that $M^*$ is responsible for the observed behavior, while QCP is formed by kinematic mechanism. It has been shown that near FCQPT, $M^*(T) \propto T^{-1/2}$, while the application of $H$ drives the system to the LFL region with $M^*(H) \propto (H_s - H)^{-1/2}$ [4, 5, 3]. At finite $H$ and $T$ near FCQPT, the solutions of Eq. (3) $M^*(T,H)$ can be well approximated by a simple universal interpolating function [4, 3, 5]. The interpolation occurs between the LFL ($M^* \propto a + bT^2$) and NFL ($M^* \propto T^{-1/2}$) regimes and represents the universal scaling behavior of $M^*_N(T_N)$ independent of spatial dimension of the considered system

$$M^*_N = \frac{1+c_2}{1+c_1} \frac{1+c_1 T_N^2}{1+c_2 T_N^{5/2}}, \quad (4)$$

where $c_1$ and $c_2$ are fitting parameters, $M^*_N = M^*/M^*_M$ and $T_N = T/T_M$ are the normalized effective mass and temperature respectively. Here,

$$M^*_M \propto (H_s - H)^{-1/2}, \quad (5)$$

$$T_M \propto H_s - H \quad (6)$$

are the maximum value of the effective mass $M^*_M$ and temperature $T_M$, corresponding to the maximum of

$(dM/dT)_{\max}(H)$ and/or $\chi_{\max}(H)$ [3, 4, 5]. Below Eq. (4) is used along with Eq. (1) to describe the experiment in CuPzN.

Taking into account that $M = \int \chi dH$ and Eqs. (4), (5), and (6), we obtain that $(M - M_s)/\sqrt{H_s - H}$ as a function of the variable $T/(H_s - H)$ exhibits scaling behavior. This result is in good agreement with the experimental facts, as it is seen from Fig. 1 that reports

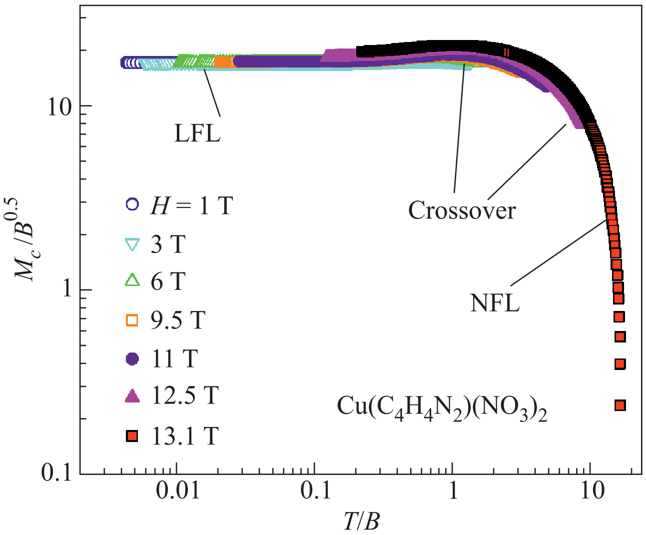


Fig. 1. (Color online) The scaling behavior of the magnetization $M_c/B^{0.5}$ versus $T/B$ at different magnetic fields $H$, shown in the legend, with $M_c = a + (M - M_s)$ and $B = H_s - H$. The LFL, crossover and NFL regions are shown by the arrows. The data are extracted from measurements [1]

the plot of the scaling behavior of the magnetization $M_c/B^{0.5} = a + (M - M_s)/(H_s - H)^{0.5}$ as a function of $T/B = T/(H_s - H)$, with $a$ is a constant added to a better presentation of the Figure. It is seen from Fig. 1, that the LFL behavior takes place at $T \ll B$, the crossover at $T \sim B$, and the NFL one at $T \gg B$, as it is in the case of HF compounds [4, 5]. It is instructive to note that the same scaling behavior exhibits $M_c$ obtained in measurements on $YbAlB_4$ under the application of magnetic field [21], see Fig. 1b of Ref. [22].

Fig. 2 portrays the comparison between $\chi_N$ extracted from the experiments on CuPzN (panel a) [1], $Au_{51}Al_{34}Yb_{15}$ quasicrystal (panel b) [23], and the theory. Here $\chi_N$ is the normalized magnetic susceptibility, while the normalization is done in the same way as it is done in the case of $M^*_N$ [4, 5]. It is seen that for more then three decades in normalized temperature there is very good agreement between the theory and the experimental data. The double log scale, used in panels a and b, reveals the universal dependence $\chi_N \sim T_N^{-0.5}$. The comparison between Fig. 2a and b indicates that $\chi_N$ of both CuPzN and the quasicrystal $Au_{51}Al_{34}Yb_{15}$ has three regions: low-temperature LFL part, medium-temperature crossover region where the maximum occurs, and high-temperature NFL part with the distinctive temperature dependence $T_N^{-0.5}$. Note that the dependences from Figs. 2a and b qualitatively resemble that of Q1D HF metal $YbNi_4P_2$ [7], and demonstrate the scaling behavior, and are similar to those of heavy-fermion compounds [3, 5]. We recall that the absolute values of the thermodynamic functions obviously depend on the interparticle interaction amplitude, therefore, to reveal the universal properties we have to employ the normalization procedure [3–5]. We note, that the approach of weakly interacting Q1DFL (1) gives for $C/T$ and $\chi$ the same high-temperature asymptotics $T^{-1/2}$.

Fig. 3a shows the normalized temperature dependence $(dM/dT)_N$ of the quantity $dM/dT$, revealing the scaling behavior, while the normalization is done in the same way as it is done in the case of $M^*_N$ or $\chi_N$. The black solid theoretical curve corresponds to the temperature derivative $dM/dT$ of the magnetization (1). Good coincidence with experiment on CuPzN is seen everywhere. Such a good agreement shows that $dM/dT$ has the universal scaling behavior, that can also be described by taking into account that $M = \int \chi dH$. In panel b of Fig. 3 the maximum values $(dM/dT)_{\max}$ of $dM/dT$ versus $H_s - H$ are displayed. The theoretical curve given by $(dM/dT)_{\max} \propto (H_s - H)^{-1/2}$ is in good agreement with experimental facts extracted from measurement of the magnetization [1], and demonstrates that the effective mass of spinons does diverge at $H \to H_s$.

The above thermodynamic properties reported in Figs. 2, 3, and 4 coincide with those of HF compounds, and permit us to construct the $T-H$ phase diagram of CuPzN, shown in Fig. 5. To do so, in Fig. 4a we report the peak temperature $T_M$ of magnetic susceptibility as a function of $H$. It is seen, that the peak temperature $T_M$ goes to zero as $H$ approaches $H_s$. In panel b of Fig. 4 the maximum values $\chi_{\max}$ of $\chi$ versus $H_s - H$ are displayed. It is seen, that theoretical curve given by Eq. (5) is in good agreement with experimental data extracted from measurement of the magnetization [1], and demonstrates that the effective mass of spinons does diverge at $H \to H_s$, as it is at FCQPT. The $T-H$ phase diagram reported in Fig. 5 demonstrates that peak dependence $T_M$ takes place over wide range of variation of $H$, for $T_M \propto H_s - H$. This shows, that main property of these lines is that they are straight lines, representing energy scales typical for HF metals located at their

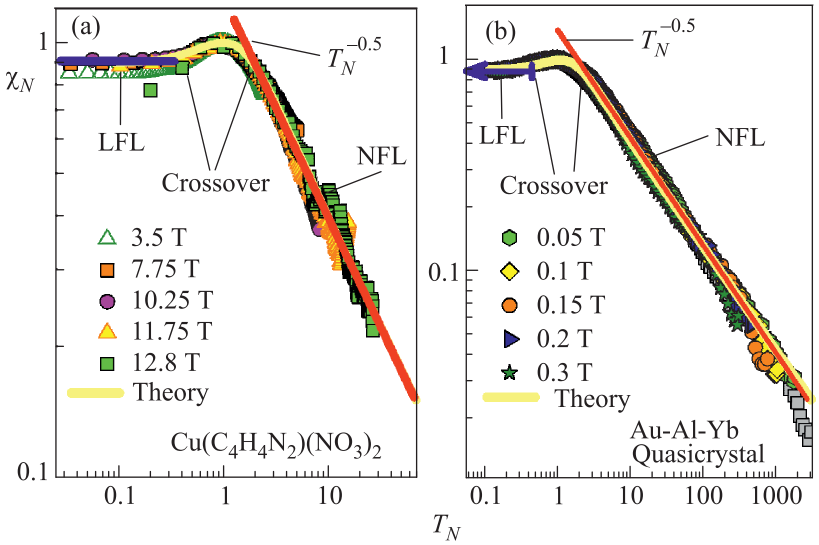


Fig. 2. (Color online) (a) – The normalized magnetic susceptibility $\chi_N$ extracted from measurements in magnetic fields $H$ (shown in the legend) on CuPzN [1] and on $Au_{51}Al_{34}Yb_{15}$ quasicrystal [23]. Our theoretical curves, merged in the scale of the Figure and plotted on the base of Eqs. (1) and (4), are reported by the solid lines tracing the scaling behavior. Panels a and b show that dependence $\chi_N(T_N)$ for CuPzN and quasicrystal has three distinctive regions: LFL, crossover and NFL, where $\chi_N \sim T_N^{-0.5}$ shown by the straight line

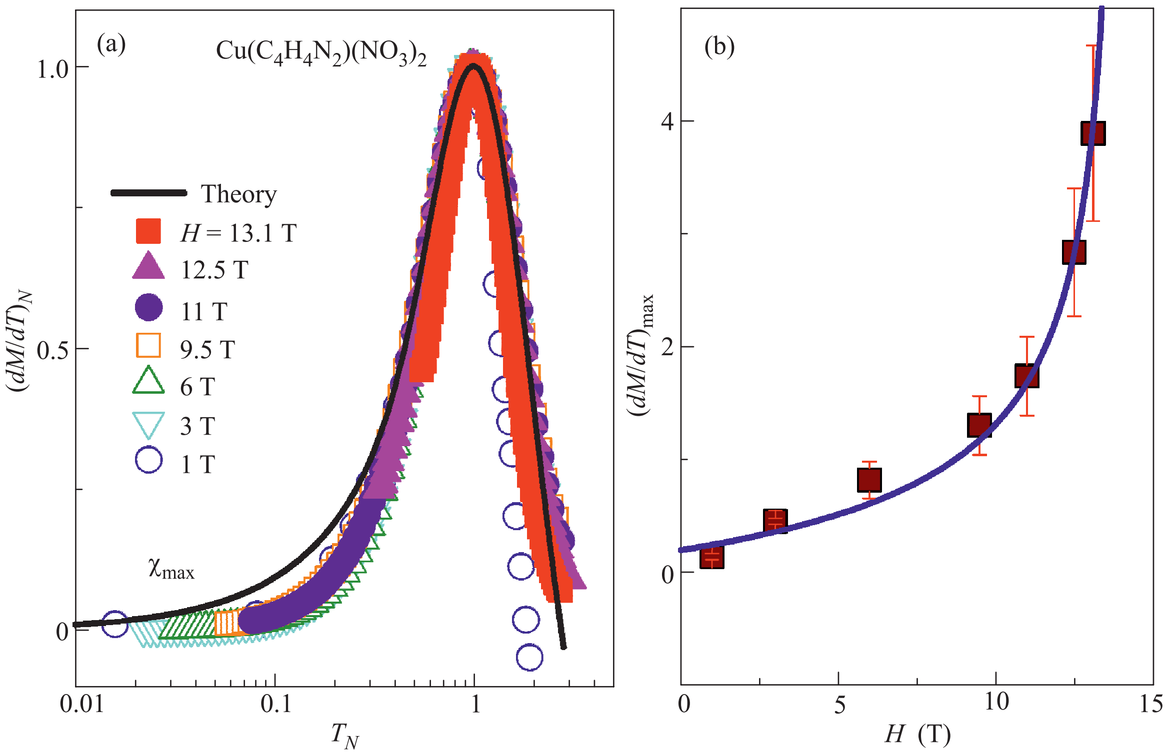


Fig. 3. (Color online) (a) – The normalized $(dM/dT)_N$ extracted from measurements in magnetic fields on CuPzN [1]. Theoretical curve, based on Eq. (1) is also reported. (b) – The magnetic field dependence of the maximum values $(dM/dT)_{\max}$ of $dM/dT$. The theoretical curve is given by $(dM/dT)_{\max} \propto (H_s - H)^{-1/2}$, see Eq. (5)

QCP [24, 25]. Since FCQPT takes place at $H = H_s$, the phase diagram is almost symmetric with respect to the point $H = H_s$, and consists of the LFL, gapped Fermi liquid, crossover and NFL regions. The crossover

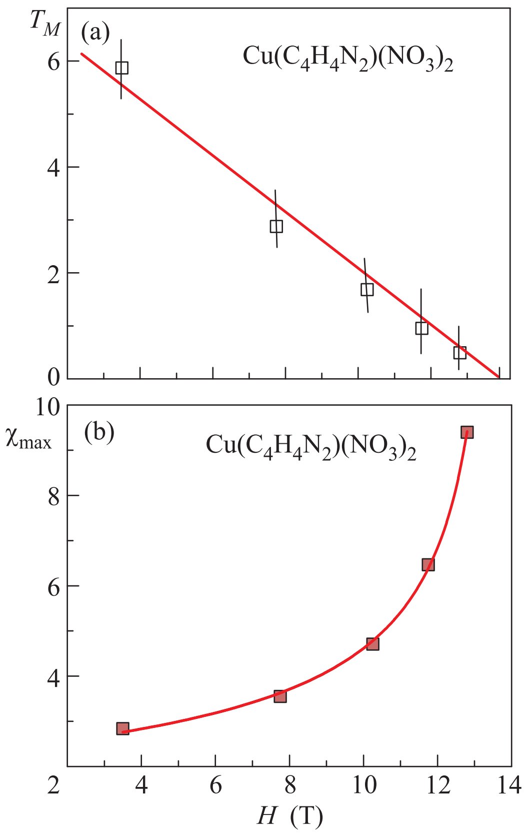


Fig. 4. (Color online) (a) – The magnetic field dependence of peak temperature $T_M$ of the magnetic susceptibility $\chi$ of CuPzN, gathered from experimental data [1]. The calculated straight line $T_M \propto H_s - H$ given by Eq. (6) demonstrates good agreement with the experimental data. (b) – The magnetic field dependence of the maximum values $\chi_{\max}(H)$. The theoretical curve is given by $\chi_{\max} \propto (H_s - H)^{-1/2}$, see Eq. (5)

regions in Fig. 5 are shown by arrows, and are formed by the straight lines, which are the magnetic field dependencies of temperatures of approximate LFL and NFL boundaries as well as by that of $T_M$. NFL state occurs at relatively high temperatures with the distinct temperature dependence $\sim T_N^{-1/2}$. At the same time LFL regions occur at low $T$, where the spinon effective mass is almost constant, as is the case for LFL behavior. At $H > H_s$ the QSL becomes a gapped field-induced paramagnetic spin liquid, as shown in Fig. 5. At rising temperatures and fixed magnetic field $H$, the system transits through the crossover, and enters the NFL region, as it is seen from Fig. 5. It is also seen, that the crossover becomes wider, as the systems moves from FCQPT shown by the filled circle. We conclude that CuPzN exhibits the behavior typical for HF compounds [25] that leads to the formation of the corresponding $T{-}H$ phase diagram displayed in Fig. 5.

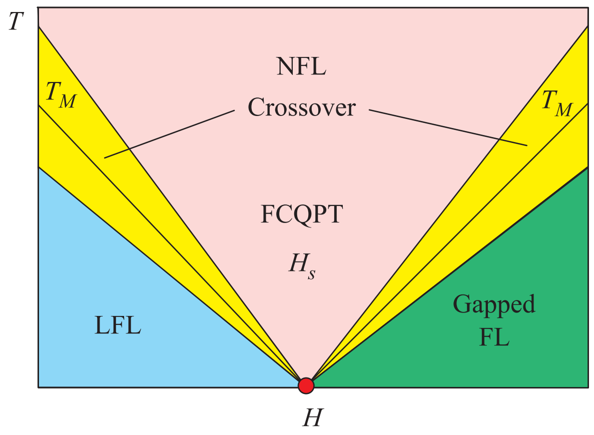


Fig. 5. (Color online) Schematic magnetic field – temperature phase diagram of CuPzN, based on data from panels a of Fig. 2 for $H \lessgtr H_s$. Straight lines on both sides of $H_s$, which is FCQPT point, indicate, respectively, the lines of LFL boundary (the lowest temperature), the temperatures of maxima (middle line, marked "$T_M$") and the end of crossover region (the highest temperature at which the system enters the NFL regime), see Fig. 2a. The right sector labeled as "gapped FL" denotes the gapped field-induced paramagnetic spin liquid

In summary, we have shown that the thermodynamic properties of CuPzN are defined by weakly interacting QSL, and explained the corresponding experimental facts. Our analysis have shown that QCP, represented by FCQPT, in CuPzN occurs due to kinematic mechanism: The band becomes approximately flat not due to interaction between fermions but rather due to the application of sufficiently strong magnetic field $H = H_s$. We have constructed the $T{-}H$ phase diagram of CuPzN and for the first time have shown that it is approximately symmetric with respect to QCP, and has the LFL part, crossover, gapped Fermi liquid, and NFL part. For the first time, we have also revealed that CuPzN exhibits the universal scaling behavior typical for HF compounds.

We thank V.A. Khodel and Y. Kono for valuable comments. V.R.S. is supported by the Russian Science Foundation, Grant # 14-22-00281. K. G. P. is partly supported by RFBR Grant # 14-02-00044 and the Saint Petersburg State University Grant # 11.38.658.2013.

1. Y. Kono, T. Sakakibara, C.P. Aoyama, C. Hotta, M.M. Turnbull, C.P. Landee, and Y. Takano, Phys. Rev. Lett. **114**, 037202 (2015).
2. D. Shechtman, I. Blech, D. Gratias, and J.W. Cahn, Phys. Rev. Lett. **53**, 1951 (1984).
3. V.R. Shaginyan, A.Z. Msezane, K.G. Popov, G.S. Japaridze, and V.A. Khodel, Phys. Rev. B **87**, 245122 (2013).

4. V. R. Shaginyan, M. Ya. Amusia, A. Z. Msezane, and K. G. Popov, Phys. Rep. **492**, 31 (2010).
5. M. Ya. Amusia, K. G. Popov, V. R. Shaginyan, and V. A. Stephanovich, *Theory of Heavy-Fermion Compounds*, Springer Series in Solid-State Sciences (2014), v. 182.
6. V. R. Shaginyan, A. Z. Msezane, and K. G. Popov, Phys. Rev. B **84**, 060401(R) (2011).
7. C. Krellner, S. Lausberg, A. Steppke, M. Brando, L. Pedrero, H. Pfau, S. Tencé, H. Rosner, F. Steglich, and C. Geibel, New J. Phys. **13**, 103014 (2011).
8. A. V. Rozhkov, Eur. Phys. J. B **47**, 193 (2005).
9. V. R. Shaginyan, A. Z. Msezane, K. G. Popov, and V. A. Stephanovich, Phys. Rev. Lett. **100**, 096406 (2008).
10. A. V. Rozhkov, Phys. Rev. Lett. **112**, 106403 (2014).
11. A. G. Lebed, Phys. Rev. Lett. **115**, 157001 (2015).
12. Y. Maeda, C. Hotta, and M. Oshikawa, Phys. Rev. Lett. **99**, 057205 (2007).
13. T. Nikuni, M. Oshikawa, A. Oosawa, and H. Tanaka, Phys. Rev. Lett. **84**, 5868 (2000).
14. I. M. Lifshitz, Sov. Phys. JETP **11**, 1130 (1960).
15. G. E. Volovik, Lect. Notes Phys. **718**, 31 (2007).
16. G. E. Volovik, Phys. Scr. T **164**, 014014 (2015).
17. V. A. Khodel, J. W. Clark, K. G. Popov, and V. R. Shaginyan, JETP Lett. **101**, 413 (2015).
18. L. D. Landau, Sov. Phys. JETP **3**, 920 (1956).
19. J. W. Clark, V. A. Khodel, and M. V. Zverev, Phys. Rev. B **71**, 012401 (2005).
20. V. A. Khodel, J. W. Clark, and M. V. Zverev, Phys. Rev. B **78**, 075120 (2008).
21. Y. Matsumoto, S. Nakatsuji, K. Kuga, Y. Karaki, N. Horie, Y. Shimura, T. Sakakibara, A. H. Nevidomskyy, and P. Coleman, Science **331**, 316 (2011).
22. Y. Matsumoto, S. Nakatsuji, K. Kuga, Y. Karaki, Y. Shimura, T. Sakakibara, A. H. Nevidomskyy, and P. Coleman, J. Phys.: Conf. Ser. **391**, 012041 (2012).
23. K. Deguchi, S. Matsukawa, N. K. Sato, T. Hattori, K. Ishida, H. Takakura, and T. Ishimasa, Nat. Mater. **11**, 1013 (2012).
24. M. Brando, L. Pedrero, T. Westerkamp, C. Krellner, P. Gegenwart, C. Geibel, and F. Steglich, Phys. Stat. Sol. B **459**, 285 (2013).
25. V. R. Shaginyan, A. Z. Msezane, K. G. Popov, G. S. Japaridze, and V. A. Khodel, Europhys. Lett. **106**, 37001 (2014).